Far-infrared c-axis response of (La, Sr)2CuO4-delta determined by ellipsometry

Henn, R.; Kircher, J.; Cardona, M.; Wittlin, A.; Duijn, V.H.M.; Menovsky, A.A.

Published in:
Physical Review. B, Condensed Matter

DOI:
10.1103/PhysRevB.53.9353

Far-infrared c-axis response of $La_{1.87}Sr_{0.13}CuO_4$ determined by ellipsometry

R. Henn, J. Kircher, and M. Cardona
Max-Planck-Institut für Festkörperforschung, Heisenbergstrasse 1, 70569 Stuttgart, Germany

A. Wittlin
High Field Magnet Laboratory, University of Nijmegen, NL-6525 ED Nijmegen, The Netherlands

V. H. M. Duijn and A. A. Menovsky
Department of Physics, University of Amsterdam, NL-1018 XE Amsterdam, The Netherlands

(Received 30 June 1995; revised manuscript received 17 January 1996)

We have measured the c-axis optical response of a large, high-quality single crystal of $La_{1.87}Sr_{0.13}CuO_4$ between 30 and 700 cm^{-1} in the 10–300 K temperature range with a far-infrared Fourier ellipsometer. Since ellipsometry provides both amplitude and phase information, we directly obtain the complex dielectric function, thereby avoiding the errors introduced by the Kramers-Kronig transformation or the reference determination. A purely algebraic treatment of our data within the two-fluid Gorter-Casimir model reveals no indication of a reduction of the normal carrier scattering rate Γ below T_c. We obtain $\Gamma \approx 130 \pm 70$ cm^{-1} and a plasma frequency for the superconducting carriers of $\omega_{ps} \approx 260 \pm 40$ cm^{-1}. Thus, assuming a weak-coupling BCS gap ($3.5k_BT_c \approx 77$ cm^{-1}, with $T_c = 31.5$ K) we conclude that the c-axis optical response of $La_{1.87}Sr_{0.13}CuO_4$ can neither be modeled within the clean nor with the dirty limit.

I. INTRODUCTION

In contrast to the optical conductivity $\tilde{\sigma}_{ab}(\omega,T)$ within the CuO_2 planes, which seems to be an almost universal function for all superconducting cuprates,[1] no systematic behavior has been found for the optical conductivity perpendicular to the CuO_2 planes.[2–9] However several cuprates, $La_{2-x}Sr_xCuO_4$ ($x=$ 0.1, 0.13, 0.16),[2] $YBa_2Cu_4O_8$,[3] $YBa_2Cu_3O_{7+\delta}$,[4–7] show, as a common feature, an edge structure in the far-infrared reflectivity, which appears only in the superconducting state. This edge is assigned to plasma oscillations of the superconducting condensate.[10] Although many theories concerning the c-axis response have been presented,[11–13] a consensus has not been reached on the underlying transport mechanism in either the normal or superconducting state. One of the reasons is that the differences in the predicted reflectance characteristics can be rather small, i.e., within the experimental error. In particular, two recent investigations of the superconducting state of $La_{2-x}Sr_xCuO_4$ provide two contradictory descriptions of essentially the same experimental reflectance spectra.[2,14] Tamasaku, Nakamura, and Uchida[2] have interpreted their data within the clean limit based on a strong decrease of the quasiparticle scattering rate below T_c. Kim *et al.*[14] assumed a dirty-limit superconductor with a large, temperature-independent quasiparticle scattering rate.

We have determined the c-axis optical response of a $La_{1.87}Sr_{0.13}CuO_4$ crystal using far-infrared ellipsometry. Ellipsometry enables us to overcome two main problems inherent to the competing normal incidence reflectance technique:[15]

(1) The reference problem. Especially for high sample reflectivities, the accuracy of the data is strongly affected by the experimenter's ability to determine the unity reflectance level.

(2) The phase problem. The phase shift upon reflection is determined by Kramers-Kronig transformation. This procedure requires accurate knowledge of the reflectance over a wide energy range (typically several eV).

We found neither of the two contradictory interpretations described above to be compatible with the additional phase information obtained using ellipsometry.

II. EXPERIMENTAL, SAMPLE, AND DATA EVALUATION

The measurements were performed with a home-built ellipsometer attached to a Bruker 113v Fourier transform IR spectrometer.[16] The quantity measured in ellipsometry is the complex reflectance ratio

$$\tilde{\rho}(\omega,\phi) = \frac{\tilde{r}_p(\omega,\phi)}{\tilde{r}_s(\omega,\phi)}, \tag{2.1}$$

where ϕ is the angle of incidence (in our experiment 80°, with a beam divergence of $\pm 1.7°$) and $\tilde{r}_p$ and $\tilde{r}_s$ are the Fresnel reflection coefficients for p- and s-polarized light, respectively.[17] The dielectric function is extracted from $\tilde{\rho}(\omega,\phi)$ by inverting the Fresnel equations:

$$\tilde{\epsilon}(\omega) = \left(\frac{1-\tilde{\rho}(\omega,\phi)}{1+\tilde{\rho}(\omega,\phi)}\right)^2 \tan^2\phi \, \sin^2\phi + \sin^2\phi. \tag{2.2}$$

The inversion given in (2.2) assumes an isotropic, clean, and homogeneous sample-ambient interface. For an anisotropic sample different dielectric tensor elements contribute to $\tilde{\rho}(\omega,\phi)$. For such a sample the formal inversion according to (2.2) yields the so-called pseudodielectric function $\langle\tilde{\epsilon}(\omega)\rangle$.[18] For a uniaxial material, like $(La,Sr)_2CuO_4$, we can obtain the dielectric tensor components $\tilde{\epsilon}^{aa}(\omega)$ and $\tilde{\epsilon}^{cc}(\omega)$ by fitting the Fresnel equations for a uniaxial material

to two experimental spectra of $\tilde{\rho}(\omega,\phi)$ (taken with the c axis parallel and perpendicular to the plane of incidence).[19,20] Our fits show that Aspnes's suggestion[21] that the pseudodielectric function is a good approximation for the dielectric tensor element along the line of intersection between the plane of incidence and the sample surface is valid for our measurements. The $\tilde{\epsilon}^c(\omega)$ data presented in this paper are pseudodielectric functions measured with the c axis along the line of intersection between the plane of incidence and the sample surface. We point out that the fit obtained using the full anisotropic tensor elements did not alter the results and only served to degrade the signal-to-noise ratio due to noisy a-axis data. In order to cover the whole frequency range from 30 to 700 cm^{-1} we took spectra with three different sets of beam splitters and filters (30–100, 80–350, 300–700 cm^{-1}) at each temperature. These curves agreed perfectly in the overlapping regions.

We investigated a $La_{1.87}Sr_{0.13}CuO_4$ single crystal grown by the traveling-solvent floating-zone method.[22] Superconducting quantum interference device magnetization measurements (field cooled and zero-field cooled), as well as transport measurements parallel and perpendicular to the CuO_2 planes, show a sharp superconducting transition at 31.5 K. In agreement with Nakamura and Uchida,[23] we observe an almost temperature-independent normal-state resistivity perpendicular to the CuO_2 planes and a linear temperature dependence of the resistivity along the CuO_2 planes. These results strongly suggest different scattering mechanisms parallel and perpendicular to the CuO_2 planes. The anisotropy ratio ρ_c/ρ_{ab} is about 200 at room temperature and increases with decreasing temperature.

The measurements were performed on a mechanically polished (100) surface. We determined the c axis of our sample with Raman scattering and x-ray diffraction in Laue geometry. The surface of the sample had a semicircular shape with a diameter of 7 mm and was illuminated completely. The thickness of the sample was about 1 mm, sufficient to make the sample opaque throughout the entire measurement range.

III. RESULTS AND DISCUSSION

The real and imaginary parts of the dielectric function, $\epsilon_1^c(\omega)$ and $\epsilon_2^c(\omega)$, are shown in Fig. 1 for two different temperatures. The spectra resemble those of an ionic insulator with phononic contributions dominating the optical response. There is, however, an additional electronic contribution present dominating the response below about 180 cm^{-1}. This electronic response is the main subject of this paper. In the inset of Fig. 1 we display the reflectance calculated from our data for several temperatures in the region where the temperature dependence is most prominent. The calculated reflectance is in excellent agreement with previously published data.[2,14] Before concentrating on the electronic response, we will briefly examine the phononic contribution to our spectra.

A. Phononic response

In the discussion of the phonons appearing in our spectra one has to keep in mind the tetragonal → orthorhombic

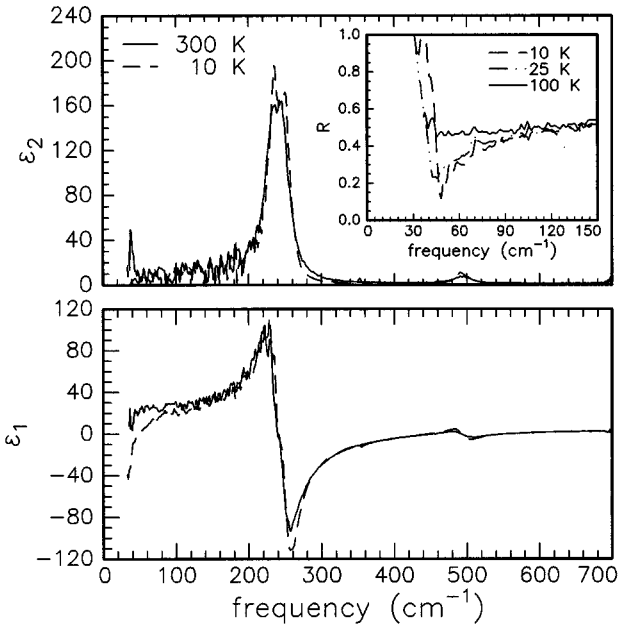

FIG. 1. The real (lower panel) and imaginary part (upper panel) of $\tilde{\epsilon}^c(\omega)$ of $La_{1.85}Sr_{0.15}CuO_4$ between 30–700 cm^{-1} at 300 K and at 10 K. The inset shows the reflectance (upper panel) between 30–150 cm^{-1} at 10, 25, and 100 K.

phase transition occurring in $La_{1.87}Sr_{0.13}CuO_4$ around 200 K:[24,25] due to the doubling of the primitive cell additional modes become infrared active in the low-temperature orthorhombic phase. This can be verified by means of the factor group analysis of the corresponding unit cells at the Γ point. The factor group analysis yields

$$\Gamma = 2A_{1g} + 4A_{2u} + B_{2u} + 2E_g + 5E_u,$$

for the tetragonal phase (*I4/mmm*) (Ref. 25) present above about 200 K and

$$\Gamma = 5A_g + 3B_{1g} + 6B_{2g} + 4B_{3g} + 4A_u + 7B_{1u} + 5B_{2u} + 8B_{3u},$$

for the orthorhombic phase (*Abma*) (Ref. 25) which exists below about 200 K. The A_{2u} and B_{1u} symmetries, respectively, allow a dipole moment parallel to the c axis and thus infrared-active modes. After subtracting the acoustic modes, the analysis yields three c-polarized (A_{2u}) infrared-active modes for the tetragonal phase and six (B_{1u}) for the orthorhombic phase.

We observe in our spectra for the tetragonal phase (300 K data in Fig. 1) two of the three predicted A_{2u} modes (at 250 and 491 cm^{-1}, the splitting of the 250 cm^{-1} mode will be discussed below). For the orthorhombic phase (10 K data in Fig. 1) we can identify four of the six expected B_{1u} modes (at 250, 312, 352, and 491 cm^{-1}). From neutron-scattering experiments the ''missing'' modes are expected at 133 cm^{-1} for the tetragonal phase[26] and at 130.4 and 145.6 cm^{-1} for the orthorhombic phase.[27] On the basis of the LO-TO splitting the oscillator strength S of these modes has been estimated to be of the order of 0.04.[27] The weak oscillator strength of these modes, together with screening effects due to the present charge carriers may prevent them from

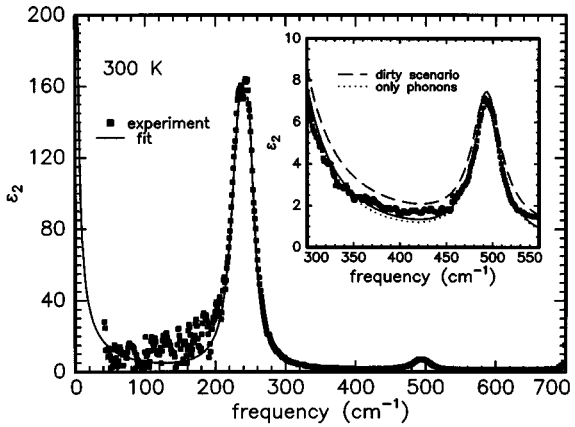

FIG. 2. Imaginary part of the c-axis dielectric function of $La_{1.87}Sr_{0.13}CuO_4$ at 300 K versus frequency (symbols) together with a fitted function. The solid line represents a fit using Lorentzians for all phonons and a Drude model for the electronic response. The fit parameters are given in Table I. The inset shows a magnification of the 300–550 cm^{-1} range. Two curves are added: the pure phononic response given by the sum of the Lorentzians of Table I (dotted line) and the phononic response with an additional Drude term given by $\omega_{p0}=1320$ cm^{-1} and $\Gamma=4670$ cm^{-1} (dashed line).

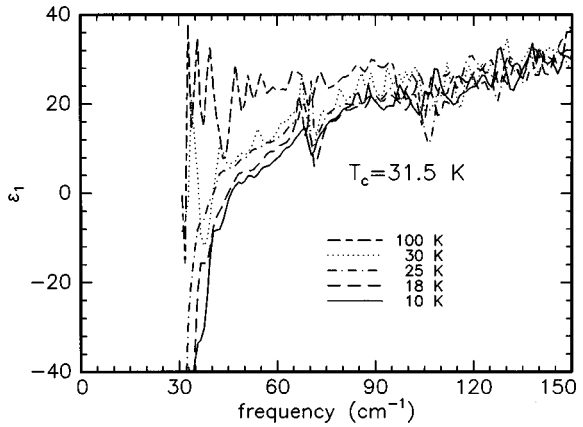

FIG. 3. Low-energy part of $\epsilon_1^c(\omega)$ for several temperatures between 10 and 100 K.

being visible in our spectra. We should also point out that no indication of these modes was found either in the reflectance data previously published.[2,14]

The line shape of the 250 cm^{-1} mode might be slightly asymmetric (Figs. 1 and 2). We could not detect any asymmetry in the other modes. Since the 250 cm^{-1} mode is attributed to the motion of La against the CuO_2 plane,[28] this mode is expected to be sensitive to the disorder in the La-Sr sublattice, for instance that resulting from the partial replacement of La by Sr. The substitution of Sr on the La sites may be the direct origin of the observed splitting of this phonon. For a weakly dispersive mode, a splitting of the phonon line with substitution, related to a phonon bound state, can be expected. Further experiments on crystals with different doping levels and dopant types will have to be performed in order to test this hypothesis.

In Fig. 2 we show the imaginary part of the dielectric function measured at 300 K (symbols) together with a phonon fit (solid line). All phonons were described by Lorentzians. In addition we included a Drude term to describe the low-frequency response ($\omega_{p0}=300$ cm^{-1}; $\Gamma=120$ cm^{-1}); this will be discussed in detail below. The parameters of the fit are given in Table I. The fit agrees well with the experimental data, a fact which is emphasized by the inset of Fig. 2 showing a magnification of the 300–550 cm^{-1} frequency range. We have added two curves to the inset: The dotted line represents the pure phononic response given by the Lorentz parameters of Table I neglecting any Drude contribution whereas the dashed line corresponds to the same Lorentz parameters plus a Drude response given by $\omega_{p0}=1320$ cm^{-1} and $\gamma=4670$ cm^{-1}. It is important to note that the phonons almost completely account for the spectral weight at these frequencies (dotted line). The Drude contribution included in the dashed line with the large scattering rate seems to be too large in the 350–550 cm^{-1} frequency range. Except for the phonon lifetime γ^{-1}, which is found to increase for all phonons with decreasing temperature, the phonon parameters are found to be fairly temperature independent. As mentioned before, the modes at 312 and 352 cm^{-1} appear only in the orthorhombic phase at low temperatures ($S_{312\,cm^{-1}}\approx 0.015$; $S_{352\,cm^{-1}}\approx 0.05$). In agreement with the weak orthorhombic distortion of the crystal, their oscillator strength is small. The 250 cm^{-1} mode, with its large oscillator strength, carries nearly all contributions to the static dielectric constant.

TABLE I. Drude (D, unscreened plasma frequency ω_i, scattering rate γ_i) and Lorentz (L, energy position ω_i, full width at half maximum γ_i, and oscillator strength S_i) parameters for the fit to the 300 K data shown in Fig. 2 ($\epsilon_\infty=4.8$).

	Oscillator			
	$L1$	$L2$	$L3$	$D1$
ω_i [cm^{-1}]	234.3	248.3	493.8	300
γ_i [cm^{-1}]	27.2	16.9	37.5	120
S_i	14.9	5.8	0.5	

B. Electronic response

Figure 3 shows the low-energy part of $\epsilon_1^c(\omega)$. At these frequencies $\epsilon_1^c(\omega)$ and $\sigma_1^c(\omega)$ are mainly determined by the electronic response of the sample. Above T_c the complex dielectric function is rather temperature independent, in agreement with the weakly temperature-dependent dc resistivity observed in this direction. The effect of the conducting carriers on $\epsilon_1^c(\omega)$ is weak because of strong scattering of the carriers by defects and phonons together with a small plasma frequency. The contribution of the absorption bands at higher frequencies to the static dielectric constant, mainly that of the 250 cm^{-1} phonon, causes $\epsilon_1^c(\omega)$ to remain positive down to the lowest measured frequency. Below T_c only a weak decrease of $\sigma_1^c(\omega)$ with temperature is observed. $\sigma_1^c(\omega)$ remains larger than zero down to the lowest measured frequency. Therefore, we have no indication for the presence of a region with zero loss. The decrease of $\sigma_1^c(\omega)$ with temperature is due to the condensation of carriers into the δ function at $\omega=0$; this δ function provides the infinite dc conductivity of the superconductor. By causality, this δ func-

tion leads to a $-\omega_{ps}^2/\omega^2$ behavior in $\epsilon_1(\omega)$ giving the inductive response of the superconducting condensate[29] and thus causing $\epsilon_1^c(\omega)$ to become negative at low frequencies. This zero crossing of $\epsilon_1^c(\omega)$ is responsible for the reflectance edge appearing in the curves measured below T_c (see inset of Fig. 1).[2,13] As the temperature is decreased, the number of condensed carriers, and thus the negative contribution to $\epsilon_1^c(\omega)$, increases, causing the plasma edge to move to higher frequencies.

After these qualitative considerations we now proceed to a more quantitative analysis of our spectra. We will first focus on the normal state, for which different descriptions have been put forth.[2,14] Based on the analysis of remarkably similar c-axis reflectance spectra, Drude models have been proposed with (unscreened) plasma frequencies of 300 cm^{-1},[2] as well as "1200 cm^{-1} or more."[14] This difference is linked to a correspondingly large difference in the scattering rates, from 165 cm^{-1} (Ref. 2) to more than 4600 cm^{-1}.[14] Consequently, it has been argued that the spectra indicate that the superconductor is in the clean limit[2] as well as in the dirty limit,[14] where the former interpretation is based on an anomalous drop of the scattering rate to $\approx$ 1 cm^{-1} below T_c. In the remainder of this paper these interpretations will be referred to as the "clean scenario" and the "dirty scenario," even when discussing the normal state. We shall base our analysis on a simple phenomenological model, however, our approach can be easily generalized to more complex mechanisms.

1. Normal state

In the normal state we assume a Drude response of the carriers at low wave numbers, as was done by both Tamasaku, Nakamura, and Uchida[2] and Kim *et al.*[14] Since we obtain $\epsilon_1^c(\omega)$ and $\epsilon_2^c(\omega)$ independently, we can determine the plasma frequency ω_{p0} and the scattering rate Γ from a purely algebraic treatment of our data. For this purpose it is instructive to plot

$$\Gamma'(\omega)=\omega\frac{\epsilon_2^c(\omega)}{\epsilon_\infty-\epsilon_1^c(\omega)}$$

and

$$\omega_{p0}'(\omega)=\omega\sqrt{\left[\left(\frac{\epsilon_2^c(\omega)}{\epsilon_\infty-\epsilon_1^c(\omega)}\right)^2+1\right][\epsilon_\infty-\epsilon_1^c(\omega)]}$$

instead of the dielectric function. These two quantities converge to the Drude model parameters ω_{p0} and Γ as $\omega\rightarrow 0$ *even* if additional contributions to the optical response are present at higher frequencies, i.e., phonons or interband transitions. ϵ_∞ accounts for the contribution of all these excitations to the static dielectric constant. In Fig. 4 we have plotted $\Gamma'(\omega)$ and $\omega_{p0}'(\omega)$ calculated from the experimentally determined dielectric function obtained at 100 and 300 K. We use $\epsilon_\infty=26$, as obtained by fitting Lorentzians to the phonons appearing in the spectra at higher frequencies (see Table I) and summing their $\omega=0$ contributions, i.e., their oscillator strengths. The open symbols correspond to our extrapolation ($\omega_{p0}=300\pm 60$ cm^{-1} and $\Gamma=120\pm 70$ cm^{-1}). We found the scattering rate Γ to be about a factor of 2 larger

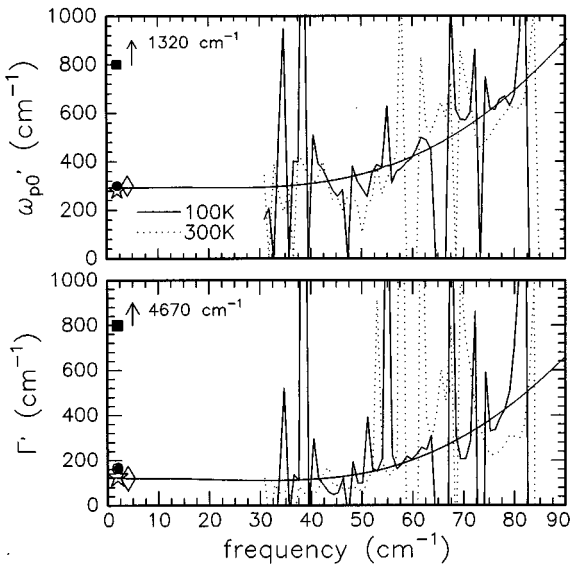

FIG. 4. $\Gamma'(\omega)$ and $\omega_{p0}'(\omega)$ using the experimentally determined dielectric functions obtained at 100 K (dotted line) and 300 K (solid line). The open symbols represent our $\omega=0$ extrapolations (star for 100 K and diamond for 300 K). The extrapolation for both temperatures is indicated by the solid lines. The solid circles and squares correspond to Drude parameters for the clean and dirty scenario found in the literature (Refs. 2 and 14).

than the screened plasma frequency, corresponding to the featureless reflectivity spectrum[12] below the reststrahlen band of the 250 cm^{-1} mode. The dc conductivity calculated from our Drude-Lorentz parameters is 12.5 $\Omega^{-1}cm^{-1}$, in excellent agreement with the measured value of 14.3 $\Omega^{-1}cm^{-1}$. The solid symbols in Fig. 4 represent the Drude parameters published for the clean and dirty scenario. The error bars are determined by estimating the uncertainty in our extrapolation. The largest source of errors in this purely algebraic treatment is the uncertainty in ϵ_∞. Since ϵ_∞ is mainly determined by the 250 cm^{-1} mode, the main source of error is the uncertainty in the description of the profile of this mode. By making a variety of different fits to the 250 cm^{-1} mode we have established $\epsilon_\infty=25.5$ to be the lower limit of ϵ_∞. Larger values of ϵ_∞ result in smaller values for Γ and $\omega_{p0}(\omega)$. Therefore, based on the assumption of a Drude response, we can clearly rule out the dirty scenario with the large scattering rate and high plasma frequency represented by the solid squares in Fig. 4. This is also completely consistent with the previously mentioned observation that, within experimental error, phonons almost completely account for the spectral weight between 300 and 550 cm^{-1}: one would expect a significant electronic contribution to the optical conductivity at these frequencies in the dirty scenario. Other scattering rates and plasma frequencies published previously for the clean scenario (solid circles in Fig. 4) agree very well with our findings.[2]

2. Superconducting state

Let us now turn our attention to the superconducting state. Based on the two-fluid Gorter-Casimir model[30]

$$\tilde{\epsilon}(\omega)=\epsilon_\infty-\frac{\omega_{ps}^2}{\omega^2}-\frac{\omega_{p0}^2-\omega_{ps}^2}{\omega(\omega+i\Gamma)},$$

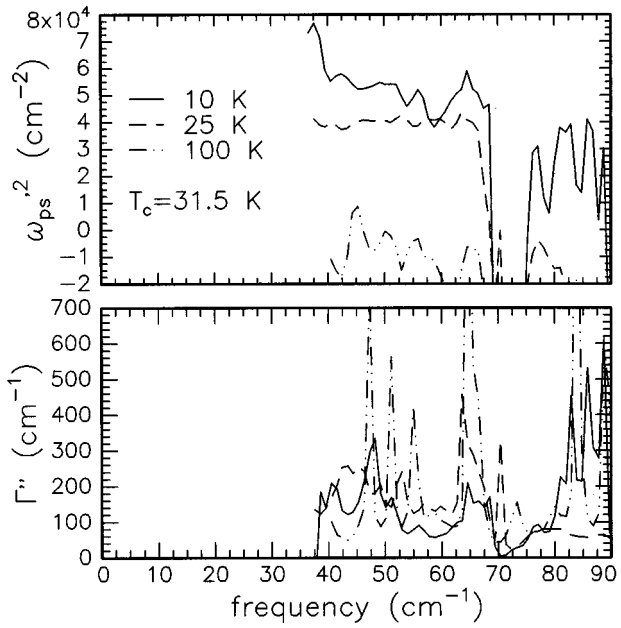

FIG. 5. $\Gamma''(\omega)$ and $\omega_{ps}'^2(\omega)$ for 10 K (solid line), 25 K (dashed line), and 100 K (dashed dotted line). Extrapolation towards $\omega \to 0$ yields Γ and ω_{ps}^2, respectively.

different sets of parameters have been proposed.[2,14] In this model ω_{ps}^2 is proportional to the number of condensed electrons whereas $\omega_{p0}^2 - \omega_{ps}^2$ corresponds to the number of "normal" quasiparticles. Since the Ferrell-Glover sum rule[31] has to be fulfilled, ω_{p0}^2 should have the same value as in the normal state. ϵ_∞ is again given by all excitations at higher energies. The two remaining parameters can be determined by plotting

$$\Gamma''(\omega) = \frac{\omega_{p0}^2 - \omega^2[\epsilon_\infty - \epsilon_1^c(\omega)]}{\omega \epsilon_2^c(\omega)},$$

and

$$\omega_{ps}'^2(\omega) = \omega^2 \left(\epsilon_\infty - \epsilon_1^c(\omega) + \frac{\epsilon_2^c(\omega)^2 \omega^2}{\omega^2[\epsilon_\infty - \epsilon_1^c(\omega)] - \omega_{p0}^2} \right)$$

which is done for several different temperatures in Fig. 5. Once again, the extrapolation $\omega \to 0$ yields the values of Γ and ω_{ps}^2, respectively. Within the experimental accuracy ω_{ps}^2 is zero above T_c (data at 100 K), indicating that the data and the algebraic treatment are meaningful. As expected, below T_c an increase of ω_{ps}^2 is seen with decreasing temperature, reflecting the enhancement of the number of condensed carriers. We observe no significant difference in the $\Gamma''(\omega)$ curves for different temperatures. The increasing noise of the $\Gamma''(\omega)$ curves below 60 cm^{-1} is attributed to the limited accuracy of the experiment at these low wave numbers. The temperature-dependent values of ω_{ps}^2 and Γ resulting from our analysis are given in Fig. 6. We see no indication for a reduction of the scattering rate below T_c, such decrease is a key ingredient for the clean scenario of Ref. 2. Assuming a weak-coupling BCS gap ($3.5 k_B T_c \approx 77$ cm^{-1}) our values for the scattering rate and for the plasma frequency ($\Gamma = 120 \pm 70$ cm^{-1} and $\omega_{ps} = 250 \pm 40$ cm^{-1} at 10 K) support neither an interpretation within the clean nor within the dirty limit.

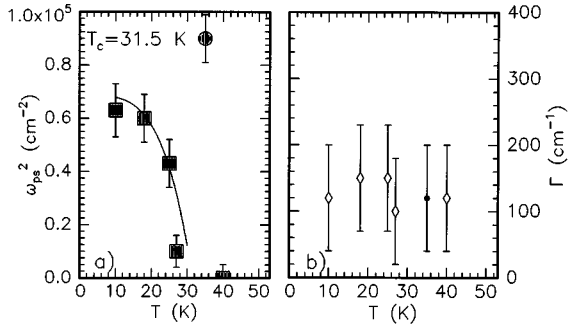

FIG. 6. ω_{ps}^2 (a) and Γ (b) versus temperature. Both sets of data are obtained by extrapolating the functions $\omega_{ps}'^2(\omega)$ and $\Gamma''(\omega)$ towards $\omega = 0$ for each temperature (see Fig. 5). For comparison we have plotted (solid circles) the values for ω_{p0} and Γ obtained by using a Drude model for the normal state (see Fig. 4). The solid line represents a least-squares fit with $\omega_{ps}^2(T) = \omega_{ps}^2(T = 0\ \mathrm{K})[1 - (T/T_c)^4]$ according to the two-fluid mode ($T_c = 31.5$ K yields $\omega_{ps} = 260$ cm^{-1}).

The extrapolation of ω_{ps}^2 towards $T = 0$ K yields a value of $\omega_{ps} = 260 \pm 50$ cm^{-1}. This means that even at $T = 0$ K the plasma frequency attributed to the superconducting condensate is smaller (by a factor of ≈ 0.87) than the plasma frequency in the normal state, where we obtained $\omega_{p0} = 300 \pm 40$ cm^{-1}. This difference reflects the fact that only the subgap spectral weight is condensed into the δ function.[1,12]

The decrease of the optical conductivity below T_c (shown in Fig. 3), or more precisely the "missing area" ($\int_0^\infty [\sigma_n(\omega) - \sigma_s(\omega)] d\omega$), is related to ω_{ps}^2 via the Ferrell-Glover sum-rule.[31] However, the missing area, mainly observed below 160 cm^{-1} in our spectra, cannot fully account for the plasma frequency ω_{ps} of the superconducting condensate. That may be partially due to spectral weight above 160 cm^{-1} condensing into the δ function as well as a less than perfect extrapolation of the conductivity towards low frequencies. We also urge the reader to recall the underlying assumptions of our data treatment, the two-fluid model as well as its ingredients, a Drude and a London fluid. They may present too much of a simplification of the experimental situation.[12] Obviously our analysis can only return parameters suitable for the underlying model.

The data treatment presented above did not take into account any interaction of the phonons with the electronic background. If such interaction is present phonon and electron contributions can only be separated if a detailed theory is available. The detailed understanding of the lattice dynamics will therefore also help to further understand the electron dynamics. The vanishing electronic contribution to the infrared optical response above 300 cm^{-1}, however, is model independent.

IV. CONCLUSION

We have measured the complex dielectric function of $La_{1.87}Sr_{0.13}CuO_4$ along the c axis by means of far-infrared

ellipsometry. The reflectance calculated from our data is in excellent agreement with the measured reflectance published by other groups. Since we measure $\epsilon_1^c(\omega)$ and $\epsilon_2^c(\omega)$ independently, we can determine the plasma frequency and the scattering rate for the normal state as well as the plasma frequency of the superconducting condensate and the scattering rate of the quasiparticles for the superconducting state algebraically. Using a Drude and a two-fluid Gorter-Casimir model, respectively, we find that neither a clean- nor a dirty-limit description of the optical response is adequate.

ACKNOWLEDGMENTS

We would like to thank D. Böhme for technical support. We thank S. Donovan and L. Genzel for numerous helpful discussions and a critical reading of the manuscript (S.D.). We would also like to acknowledge the transport and magnetization measurements by R.K. Kremer and E. Brücher. The work at the Max-Planck-Institute was funded in part by the European Union (Human Capital and Mobility Programme, Grant No. ERBSCI*CT910751) and by the Verband der Chemischen Industrie.

[1] For a review, see D.B. Tanner and T. Timusk, in *Physical Properties of High Temperature Superconductors III*, edited by D.M. Ginsberg (World Scientific, Singapore, 1992), p. 363, and references therein.

[2] K. Tamasaku, Y. Nakamura, and S. Uchida, Phys. Rev. Lett. **69**, 1455 (1992).

[3] D.N. Basov, T. Timusk, B. Dabrowski, and J.D. Jorgensen, Phys. Rev. B **50**, 3511 (1994).

[4] R.T. Collins, Z. Schlesinger, F. Holtzberg, and C. Feild, Phys. Rev. Lett. **63**, 422 (1989).

[5] M. Bauer, Ph.D. thesis, University of Tübingen, 1990.

[6] C.C. Homes, T. Timusk, R. Liang, D.A. Bonn, and W.N. Hardy, Phys. Rev. Lett. **71**, 1645 (1993).

[7] J. Schützmann, S. Tajima, S. Miyamoto, and S. Tanaka, Phys. Rev. Lett. **73**, 174 (1994).

[8] J. Kircher, M. Cardona, M. Garriga, B. Nick, M. Dürrler, A. Zibold, and H.P. Geserich, Physica C **174**, 377 (1991).

[9] J.H. Kim, I. Bozovic, D.B. Mitzi, A. Kapitulnik, and J.S. Harris, Jr., Phys. Rev. B **41**, 7251 (1990).

[10] M.S. Sherwin, P.L. Richards, and A. Zettl, Phys. Rev. B **37**, 1587 (1988).

[11] D.G. Clarke, S.P. Strong, and P.W. Anderson, Phys. Rev. Lett. **74**, 4499 (1995).

[12] S.V. Pokrovsky and V.L. Pokrovsky, J. Supercond. **8**, 183 (1995).

[13] M. Tachiki, T. Koyama, and S. Takahashi, Phys. Rev. B. **50**, 7065 (1994).

[14] J.H. Kim, H.S. Somal, D. van der Marel, A.M. Gerrits, A. Wittlin, V.H.M. Duijn, N.T. Hien, and A.A. Menovsky, Physica C **247**, 297 (1995).

[15] D. Miller and P.L. Richards, Phys. Rev. B **47**, 12 308 (1993).

[16] K.L. Barth, D. Böhme, K. Kamaras, F. Keilmann, and M. Cardona, Thin Solid Films **234**, 314 (1993).

[17] R.M.A. Azzam and N.M. Bashara, *Ellipsometry and Polarized Light* (North-Holland, Amsterdam, 1977).

[18] D.E. Aspnes, J. Opt. Soc. Am. **70**, 1275 (1980).

[19] S. Logothetidis, M. Cardona, P. Lautenschlager, and M. Garriga, Phys. Rev. B **34**, 2458 (1986).

[20] J. Kircher, M. Alouani, M. Garriga, P. Murugaraj, J. Maier, C. Thomsen, M. Cardona, O.K. Andersen, and O. Jepsen, Phys. Rev. B **40**, 7368 (1989).

[21] D.E. Aspnes, J. Opt. Soc. Am. **62**, 1175 (1972).

[22] I. Tanaka and H. Kojima, Nature (London) **337**, 21 (1989).

[23] Y. Nakamura and S. Uchida, Phys. Rev. B **47**, 8369 (1993).

[24] D.T. Keane, G.A. Held, J.L. Jordan-Sweet, M.W. Shafer, P.M. Horn, G. Güntherodt, J. Langen, M. Weit, A. Erle, S. Blumenroder, and E. Zirngiebl, Physica C **153-155**, 594 (1988).

[25] W.H. Weber, C.R. Peters, and E.M. Logothetis, J. Opt. Am. B **6**, 455 (1989).

[26] L. Pintschovius, N. Pyka, W. Reichardt, A.Yu. Rumiantsev, N.L. Mitrofanov, A.S. Ivanov, G. Collin, and P. Bourges, Physica C **185-189**, 156 (1991).

[27] W. Reichardt (private communication).

[28] M. Mostoller, J. Zhang, A.M. Rao, and P.C. Eklund, Phys. Rev. B **41**, 6488 (1990).

[29] M. Tinkham, *Introduction to Superconductivity* (McGraw-Hill, New York, 1975).

[30] D. van der Marel, H.U. Habermeier, D. Heitmann, W. König, and A. Wittlin, Physica C **176**, 1 (1991).

[31] R.A. Ferrell and R.E. Glover III, Phys. Rev. **109**, 1398 (1958).